THE JOURNAL OF PHYSICAL CHEMISTRY Letters

Letter

pubs.acs.org/JPCL

Microfluidics Reveals a Flow-Induced Large-Scale Polymorphism of Protein Aggregates

Vito Foderà,*[,†] Stefano Pagliara,[†] Oliver Otto,[‡] Ulrich F. Keyser,[†] and Athene M. Donald[†]

[†]Sector of Biological and Soft Systems, Department of Physics, Cavendish Laboratory, University of Cambridge, JJ Thomson Avenue, Cambridge CB3 0HE, United Kingdom

[‡]Biotechnology Center, Technische Universität Dresden, 01062 Dresden, Germany

Supporting Information

ABSTRACT: Amyloid fibrils are characterized by a structural arrangement of cross β-sheet as a common motif. However they can also experience a more complicated packing into a variety of 3D supramolecular structures (polymorphism). Confinement and flow rate play a crucial role in protein aggregation in living systems, but controlling such parameters during in vitro experiments still remains an unsolved problem. Here we present evidence of the effect of flow rate on the aggregation process in a confined environment using microfluidics. Specifically, we show that a gradual transition from spherical aggregates, that is, spherulites, to thick fiber-like structures takes place as a result of increasing the flow rate. Such results have implications both for a basic understanding of the mechanism behind aggregation phenomena and in the development of novel biomaterials.

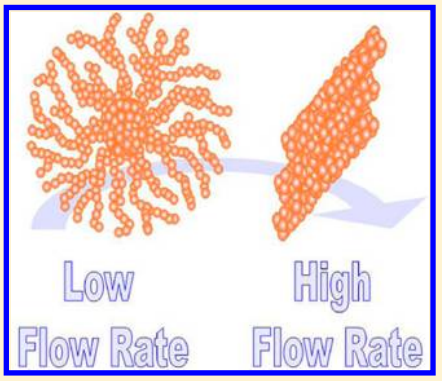

SECTION: Biophysical Chemistry and Biomolecules

Undergoing a non-native self-assembly reaction is a possible and general pathway for many proteins and peptides.[1,2] Such aggregation processes are mainly related to high-impact neurodegenerative diseases such as Alzheimer's and Parkinson's, in which the role of elongated aggregates (i.e., amyloid fibrils) is still a matter of debate.[3,4] Moreover, fibrils present peculiar properties such as size and structure that suggest their exploitation as new biocompatible materials for bionanotechnology and nanomedicine.[5]

Single amyloid fibrils are only one of the possible final results of an aggregation reaction. In fact, fibrils may generally preserve their basic structural arrangement of cross β-sheet yet experience different packing into 3D supramolecular structures (*macroscopic polymorphism*).[6,7] Interestingly, different morphologies could be associated with a variety of biological activities.[8] Therefore, understanding which factors determine the growth of a specific morphology is crucial.

Most of the current scientific activities are focused on studies performed in bulk solution. On the one hand, such an approach gives the opportunity to tune physicochemical parameters of the solution (e.g., pH, protein concentration, and salt), providing key information about some of the molecular mechanisms behind aggregation reactions.[9−11] On the other hand, such studies do not include the possibility for a geometrical confinement of the protein molecule in a flow regime, which is a typical scenario for in vivo protein aggregation.[12] As a consequence, fully mimicking in vivo conditions during in vitro experiments still represents a challenging task with a broad relevance that spans from biophysics to medicine, where this knowledge is urgently needed.[12]

Here we exploit microfluidic channels to study the effect of flow rate on protein aggregation reaction in a confined environment with a focus on its effect on the final large-scale aggregate morphology. Specifically, we prove for the first time that the aggregate morphology undergoes a transition from spherical aggregates (amyloid spherulites) and thin fibrils to elongated superstructures as a direct consequence of the increasing flow rate. We characterize such superstructures by cross-polarized and fluorescence microscopy, Fourier-transform infrared spectroscopy (FTIR), and scanning electron microscopy (SEM), revealing a fiber-like arrangement with a significant content of β-sheet structures.

The effect of shear force on protein stability has been studied using different approaches, such as a Couette setup,[13,14] mechanical shaking of the sample holder, and stirring the protein solution.[14,15] Such approaches have mainly led to the conclusion that shear force accelerates the rate of fibril formation.[13] Interestingly, the capability of shear fields to drive the unfolding of the native structure was suggested for Aβ peptide with the formation of single amyloid fibrils being favored at high shear rate.[15,16] Moreover, the shear-induced formation of conformationally different amyloid fibrils (*microscopic polymorphism*) has been reported for insulin, pointing to

Received: September 9, 2012
Accepted: September 12, 2012
Published: September 12, 2012

the potential effect of this parameter on both the microscopic fibril morphology and specific chemical properties of fibrils.[17,18] However, how the large-scale arrangement of aggregates of amyloid assemblies (μm range) is influenced by shear fields is still not clear. This lack of knowledge is partially due to the fact that the above-mentioned methods do not allow for either quantitative control of the flow rate in a confined environment or a real-time morphological investigation. Moreover, in most of these settings the flow is highly heterogeneous in the sample volume, providing poorly controlled shear conditions that are difficult to quantify.[19,20]

Microfluidic setups can process small amounts of fluid in a laminar flow regime within channels ranging from a few to some hundreds of micrometers in width and height.[21] These advantages lead to a wide use of microfluidics in cell biology,[22] drug delivery,[21] and screening.[23] The possibility of inducing protein aggregation in microchannels was previously reported by Lee and coworkers,[24−26] and recently a microdroplet assay has been shown to be effective in studying the early stages of the aggregation process.[27]

In this letter, we use insulin as a model system. The aggregation processes of this protein are also of practical importance within the context of controlling the stability of formulations in diabetes treatments.[27] Samples were prepared in HCl solution (pH 1.75) at a protein concentration of 1 mg/mL (see Supporting Information, SI). We preliminarily investigated the aggregation process under quiescent conditions and in the absence of confinement. After 24 h of incubation at 60 °C, proteins aggregate and form thin elongated fibrils and spherical aggregates, that is, amyloid spherulites (see Figure S1 in the SI). In agreement with previous reports, spherulites with an average radius of ∼20 μm are the dominant species,[28] and they are easily detectable using environmental scanning electron microscopy (ESEM, see Figure S1a,b in the SI) and cross-polarized microscopy.[28] To monitor aggregation under controlled shear flow, we then investigated the aggregation process in microfluidic channels. Figure 1 shows a schematic of the experimental setup used for our experiments.

A solution of native insulin was injected at controlled flow rates (in the range 0.1 to 1 μL/min) into the microfluidic chip,

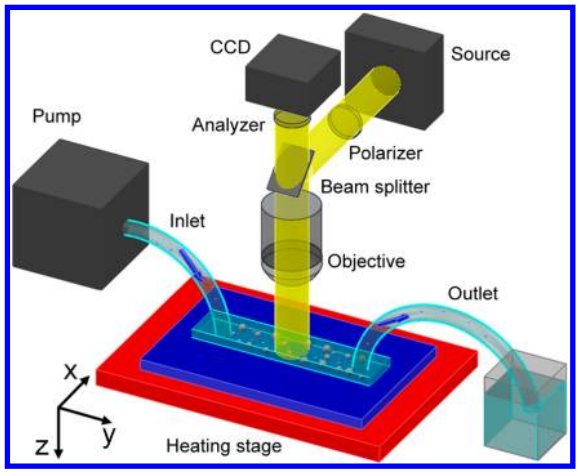

Figure 1. Experimental setup for the investigation of the flow-induced polymorphism. Native protein solution is injected into the microfluidic chip via a pump. The chip temperature is kept at 60 °C using a heating stage. Protein aggregation is followed in real time by cross-polarized optical microscopy.

and time-lapse cross-polarized optical microscopy analysis was performed in the $x-y$ plane. The temperature in the polydimethylsiloxane (PDMS) microfluidic device (see the SI for fabrication details) was controlled through a programmable heating stage set to 60 °C (Figure 1). The design of the channel allowed for confinement in the z direction (∼16 μm in height), whereas the width (x axis) and the length (y axis) were 1 mm and 1 cm, respectively (see the SI).

In the regime of low flow rate (0.1 μL/min) and after 24 h of injection in the heated device, cross-polarized images reveal the well-known Maltese cross pattern of amyloid spherulites[7] (Figure 2a) with the first spherulites already occurring after ∼300 min (see Figure S2a in the SI).

This result resembles the observation obtained under quiescent conditions (Figure S1a,b in the SI), with a massive occurrence of such spherical aggregates. Interestingly, using quantitative image analysis, significant differences in the average radius of spherulites are detectable depending on the area of the channel. Diameters of spherulites within 100 μm of the edges of the channel show an average value of 29 ± 3 μm (Figure 2b), whereas spherulites within the central part of the channel are significantly smaller (20 ± 3 μm, Figure 2c). Moreover, the spherulites' shape deviates from a perfect sphere, especially in the central part of the channel, and some of them present a rather evident ellipsoidal appearance in the $x-y$ plane (inset in Figure 2c). Using ComSol simulations, we calculate the flow velocity along the channel (see Figure S2b in the SI). In proximity of the edge, the profile clearly shows a drop of the velocity compared with the central part of the channel. This evidence could, in principle, account for the differences in size and shape between spherulites of different areas, suggesting a change in the aggregate morphology at increasing flow rate.

To test this further, we performed two experiments at higher flow rates while keeping all other experimental parameters unchanged. At a flow rate of 0.5 μL/min, only a few spherulites appear in the channel at the end of the kinetics (∼800 min, arrows in Figure 2d). Moreover, birefringent areas can be seen in the central part of the channel (Figure 2d). Such areas are already present after ∼300 min, and their intensity grows over time following a three-step process with a plateau at ∼800 min (Figure S3a,b in the SI). At an even higher flow rate (1 μL/min) no significant occurrence of spherulites is detected, and at the end of the kinetics only highly birefringent superstructures are present (Figure 2e). The latter occur already after 150 min, and the birefringence grows along the channel until a plateau is reached at ∼400 min (see Figure S3a,c in the SI). Under the action of mechanical stirring, thin elongated fibrils tend to align laterally to form bundles of fibrils.[17] In our system, an increase in the flow rate combined with the confinement of the system both prevents the formation of spherical aggregates and favors the formation of different superstructures. Importantly, for the experiments at 0.1 and 0.5 μL/min, even longer injection/incubation times (up to 3 days) never lead to the development of the superstructures of Figure 2e (data not shown). Moreover, it is worth noting that in the quiescent regime, even at very high concentrations, solutions of insulin undergoing aggregation do not result in the formation of the structures as observed in Figure 2e.[29] This all suggests that the applied flow rate and the accompanying shear force play a major role in the drastic change in morphology observed in Figure 2.

The secondary structure of the clusters observed under 1 μL/min flow rate was investigated by Thioflavin T (ThT)

dx.doi.org/10.1021/jz301375d | J. Phys. Chem. Lett. 2012, 3, 2803−2807

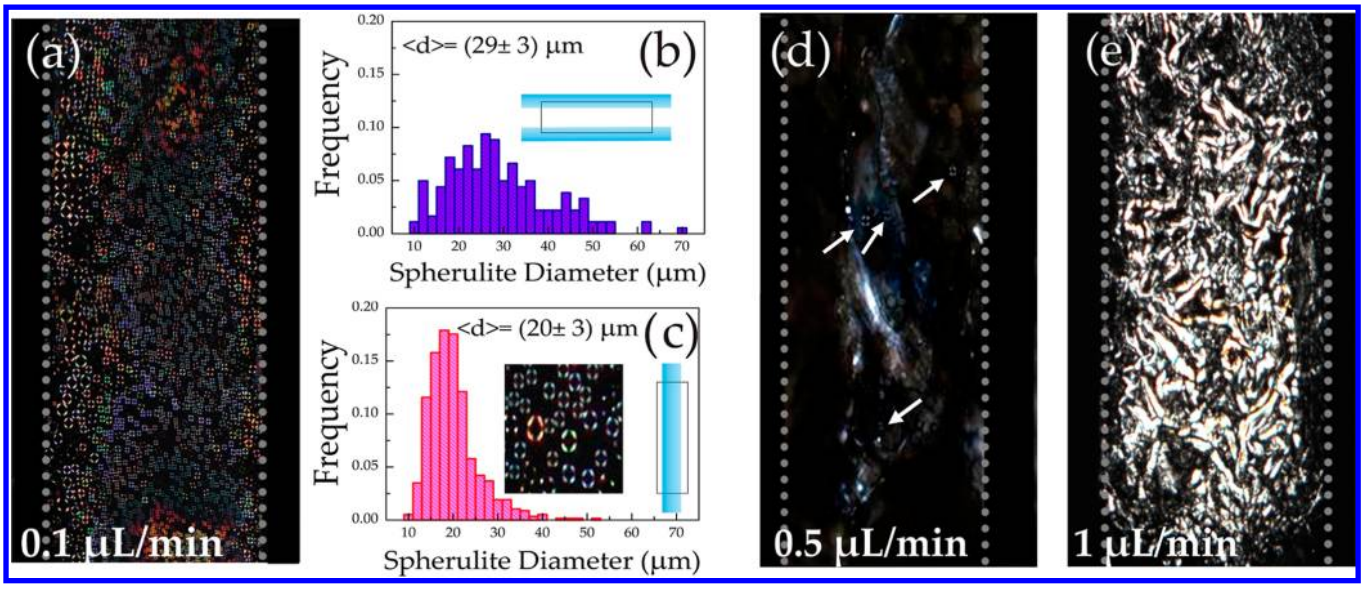

Figure 2. Cross-polarized optical microscopy images at the end of the aggregation kinetics for 1 mg/mL bovine insulin pH 1.75 at 60 °C. (a) Spherulites formed after 24 h of incubation under 0.1 μL/min flow rate. Distribution of spherulite diameters (b) close to the edges and (c) in the central part of the channel for spherulites formed at 0.1 μL/min flow rate. (d) 0.5 μL/min flow rate after 800 min and (e) 1 μL/min flow rate after 400 min. Dotted lines in panels a, d, and e highlight the channel lateral walls (1 mm width). Arrows in panel d indicate spherulites.

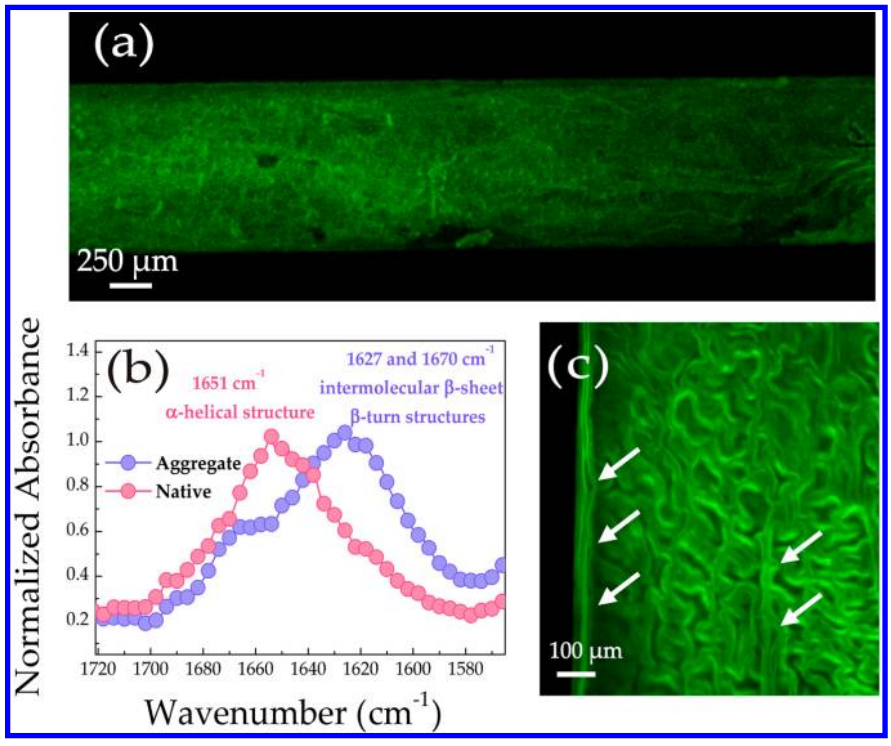

Figure 3. (a) Thioflavin T fluorescence of aggregates obtained after incubation at 60 °C under 1 μL/min flow. (b) FTIR-ATR of native structure (red) and aggregates obtained under 1 μL/min flow (blue). (c) High-magnification view of the structures. Arrows indicate fibers aligned with the flow.

staining[30−32] and ex situ FTIR (ATR configuration). Fluorescence microscopy analysis of the channel after 400 min shows a brightly fluorescent ThT signal (Figure 3a).

This proves that the observed superstructures are able to bind to ThT, suggesting the presence of β-sheet cavities available for the binding.[30] This has been further corroborated by FTIR investigation of these superstructures that reveals an enrichment in intermolecular β-sheet (1627 cm^{-1}) and β-turn structures (1670 cm^{-1})[33] with no evidence of native α-helical structure (1651 cm^{-1}, Figure 3b). This clearly indicates that the flow acts on a higher hierarchical level: large-scale packing is strongly modulated by the flow rate, whereas the building blocks of the aggregates are still characterized by a high content of β-sheets. A higher magnification image shows the appearance of the superstructures: worm-like morphology together with fibers in the range of several micrometers can be distinguished (Figure 3c). Moreover, ThT fluorescence shows that some of the structures are aligned with the flow, resembling what has

dx.doi.org/10.1021/jz301375d | J. Phys. Chem. Lett. 2012, 3, 2803−2807

previously been observed with collagen fibers in microchannels.[34] Interestingly, in our system the aligned structures are mainly localized in the central part and at the edge of the channel (arrows in Figure 3c).

We then used SEM to single out structural details of the observed superstructures. Very thick and long fibers are detected with length up to ~100 μm and thickness of several micrometers (Figure 4a,b) together with randomly oriented aggregates (arrows in Figure 4a and higher magnification in Figure 4c).

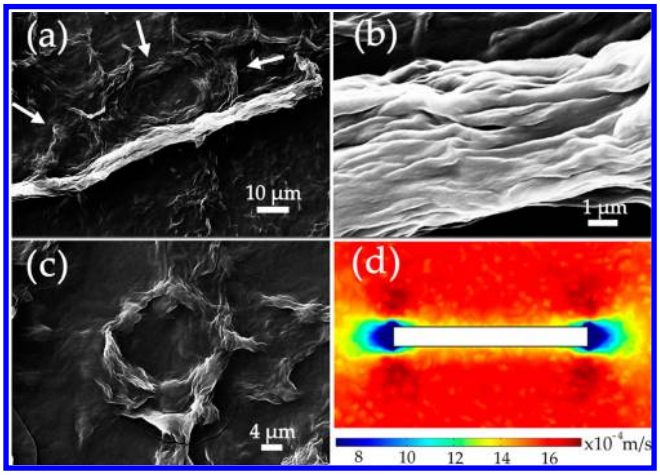

Figure 4. (a) SEM images of elongated fibers and randomly oriented aggregate close to the fiber surface (indicated by arrows) obtained under 1 μL/min flow. (b) Higher magnification view of the fiber and of (c) randomly oriented aggregates. (d) Simulation of the velocity profile along the channel at 1 μL/min and in the presence of a 100 μm long stationary object (white rectangle). The velocity scale corresponds to shear rates from 10 (dark blue) to 500 s^{-1} (dark red).

The former fibers could be imagined to form by a variety of routes: the coalescence of thin fibrils, subsequent addition of single protein molecules, or further association of disrupted fibrils. However, they are not observed under quiescent conditions, where the length and thickness of amyloid fibrils are in the range of few micrometers and nanometers, respectively (see Figure S1c,d in the SI). Regarding the randomly oriented aggregates, their origin could be related to the highly stochastic nature of insulin aggregation process.[35] Few stable aggregates are generally formed in the early stages affecting the ongoing process.[11] Under flow, once they are formed they could affect the map of velocities within the channel. Simulation in the presence of a stationary object indeed shows deviations from the laminar flow close to the object surface (Figure 4d). Such a scenario can likely be the case in our system, and irregularity in the flow can potentially modify the further growth, favoring the onset of randomly oriented aggregates, as observed in Figure 4a,c.

Our data show that geometrical confinement and flow rate in microfluidics control the aggregate morphology type. In the quiescent regime, amyloid spherulites and (thin) amyloid fibrils are formed, whereas increasing the flow rate in a confined geometry leads to the formation of clusters of very thick fibers. The flow rate affects the 3D packing of the final aggregate but leaves the structural β-sheet arrangement as a constant. These findings match recent reports suggesting that an abrupt and highly cooperative collapse of early stage filaments can occur in the presence of intensive agitation.[17] Importantly, our results also show that the shape of large spherical aggregates (i.e., spherulites) can radically change as an effect of the shear flow.

Our work provides an experimental tool for mimicking in vivo conditions during in vitro experiments. In fact, hydrodynamic flows of physiological fluids,[12] geometric confinement of the molecules,[36] and interaction of proteins with surfaces with different characteristics[37] are key factors in the development of in vivo protein aggregation and in determining the course of pathogenesis. Our well-controlled and low-cost experimental setup allows one to simultaneously control all of the above-mentioned parameters. We show that microfluidic technology coupled to numerical simulations can be easily used to study the quantitative effect of shear flow on the aggregate morphologies. However, controlling the fabrication of the channel and the coating of its internal surfaces easily offers the possibility of systematically studying the effect of different degrees of confinement in the presence of either hydrophobic or hydrophilic surfaces.

Finally, our findings may also have implications for controlling the production of novel biomaterials. Amyloid fibrils have potential in a variety of biotechnology applications.[38] However, realization of amyloid-based devices is limited by the lack of control over the morphology and alignment, both crucial for applications.[38,39] Our results show how the size of the fibers can potentially be modified by the flow rate, providing a new framework in which to rationalize and control the processing of these technological relevant materials.

■ EXPERIMENTAL METHODS

Bovine insulin was obtained from Sigma Aldrich (I5500) and dissolved at 1 mg/mL protein concentration in solution at pH 1.75 (see SI for details), and experiments were performed as shown in Figure 1. Please refer to the SI for full details of sample preparation, device fabrication, theoretical simulations, and experimental techniques.

■ ASSOCIATED CONTENT

Ⓢ Supporting Information

Details of sample preparation, device fabrication, and experimental techniques. This material is available free of charge via the Internet at http://pubs.acs.org

■ AUTHOR INFORMATION

Corresponding Author

*E-mail: vf234@cam.ac.uk.

Funding

Funding from the EPSRC (EP/H004939/1) is acknowledged. U.F.K. and S.P. acknowledge support from an ERC starting grant.

Notes

The authors declare no competing financial interest.

■ ACKNOWLEDGMENTS

We thank J. J. Rickard (University of Cambridge) for the help with TEM and ESEM experiments.

■ REFERENCES

(1) Fandrich, M.; Dobson, C. M. The Behaviour of Polyamino Acids Reveals an Inverse Side Chain Effect in Amyloid Structure Formation. *EMBO J.* **2002**, *21*, 5682−5690.

(2) Goers, J.; Permyakov, S. E.; Permyakov, E. A.; Uversky, V. N.; Fink, A. L. Conformational Prerequisites for α-Lactalbumin Fibrillation. *Biochemistry* **2002**, *41*, 12546−12551.
(3) Chiti, F.; Webster, P.; Taddei, N.; Clark, A.; Stefani, M.; Ramponi, G.; Dobson, C. M. Designing Conditions for In Vitro Formation of Amyloid Protofilaments and Fibrils. *Proc. Natl. Acad. Sci. U. S. A.* **1999**, *96*, 3590−3594.
(4) Vendruscolo, M.; Zurdo, J.; MacPhee, C. E.; Dobson, C. M. Protein Folding and Misfolding: a Paradigm of Self-Assembly and Regulativity in Complex Biological Systems. *Philos. Trans. R. Soc. London, Ser. A* **2003**, *361*, 1205−1222.
(5) Gras, S. L. Amyloid Fibrils: From Disease to Design. New Biomaterial Applications for Self-Assembling Cross-Fibrils. *Aust. J. Chem.* **2007**, *60*, 333−342.
(6) Loksztejn, A.; Dzwolak, W. Noncooperative Dimethyl Sulfoxide-Induced Dissection of Insulin Fibrils: Toward Soluble Building Blocks of Amyloid. *Biochemistry* **2009**, *48*, 4846−4851.
(7) Foderà, V.; Donald, A. M. Tracking the Heterogeneous Distribution of Amyloid Spherulites and Their Population Balance with Free Fibrils. *Eur. Phys. J. E: Soft Matter Biol. Phys.* **2010**, *33*, 273−282.
(8) Griffin, M. D.; Mok, M. L.; Wilson, L. M.; Pham, C. L.; Waddington, L. J.; Perugini, M. A.; Howlett, G. J. Phospholipid Interaction Induces Molecular-Level Polymorphism in Apolipoprotein C-II Amyloid Fibrils via Alternative Assembly Pathways. *J. Mol. Biol.* **2008**, *375*, 240−256.
(9) Vetri, V.; D'Amico, M.; Foderà, V.; Leone, M.; Ponzoni, A.; Sberveglieri, G.; Militello, V. Bovine Serum Albumin Protofibril-like Aggregates Formation: Solo but not Simple Mechanism. *Arch. Biochem. Biophys.* **2011**, *508*, 13−24.
(10) Knowles, T. P.; Waudby, C. A.; Devlin, G. L.; Cohen, S. I.; Aguzzi, A.; Vendruscolo, M.; Terentjev, E. M.; Welland, M. E.; Dobson, C. M. An Analytical Solution to the Kinetics of Breakable Filament Assembly. *Science* **2009**, *326*, 1533−1537.
(11) Foderà, V.; van de Weert, M.; Vestergaard, B. Large-Scale Polymorphism and Auto-Catalytic Effect in Insulin Fibrillogenesis. *Soft Matter* **2010**, *6*, 4413−4419.
(12) Mucchiano, G. I.; Häggqvist, B.; Sletten, K; Westermark, P. Apolipoprotein A-1-Derived Amyloid in Atherosclerotic Plaques of the Human Aorta. *J. Pathol.* **2001**, *193*, 270−275.
(13) Hill, E. K.; Krebs, B.; Goodall, D. G.; Howlett, G. J.; Dunstan, D. E. Shear Flow Induces Amyloid Fibril Formation. *Biomacromolecules* **2006**, *7*, 10−13.
(14) Bekard, I. B.; Barnham, K. J.; White, L. R.; Dunstan, D. E. α-Helix Unfolding in Simple Shear Flow. *Soft Matter* **2011**, *7*, 203−210.
(15) Hamilton-Brown, P.; Bekard, I. B.; Dunstan, D. E. How Does Shear Affect Abeta Fibrillogenesis? *J. Phys. Chem. B* **2008**, *112*, 16249−16252.
(16) Dunstan, D. E.; Hamilton-Brown, P.; Asimakis, P.; Ducker, W. Bertolini, Shear Flow Promotes Amyloid-Beta Fibrilization. *Protein Eng., Des. Sel.* **2009**, *22*, 741−746.
(17) Loksztejn, A.; Dzwolak, W. Vortex-Induced Formation of Insulin Amyloid Superstructures Probed by Time-Lapse Atomic Force Microscopy and Circular Dichroism Spectroscopy. *J. Mol. Biol.* **2010**, *395*, 643−655.
(18) Bekard, I. B.; Dunstan, D. E. Shear-Induced Deformation of Bovine Insulin in Couette Flow. *J. Phys. Chem. B* **2009**, *113*, 8453−8457.
(19) Cannon, D. Ph.D. Thesis, University of Cambridge, 2011.
(20) Bekard, I. B.; Asimakis, P.; Bertolini, J.; Dunstan, D. E. The Effects of Shear Flow on Protein Structure and Function. *Biopolymers* **2011**, *95*, 733−745.
(21) Whitesides, G. M. The Origins and the Future of Microfluidics. *Nature* **2006**, *442*, 368−373.
(22) Hung, P. J.; Lee, P. J.; Sabounchi, P.; Lin, R.; Lee, L. P. Continuous Perfusion Microfluidic Cell Culture Array for High-Throughput Cell-Based Assays. *Biotechnol. Bioeng.* **2005**, *89*, 1−8.
(23) Pagliara, S.; Chimerel, C.; Langford, R.; Aarts, D. G. A. L.; Keyser, U. F. Parallel Sub-Micrometre Channels with Different Dimensions for Laser Scattering Detection. *Lab Chip* **2011**, *11*, 3365−3368.
(24) Lee, J. S.; Um, E.; Park, J. K.; Park, C. B. Microfluidic Self-Assembly of Insulin Monomers into Amyloid Fibrils on a Solid Surface. *Langmuir* **2008**, *24*, 7068−7071.
(25) Lee, J. S.; Park, C. B. Microfluidic Dissociation and Clearance of Alzheimer's Beta-Amyloid Aggregates. *Biomaterials* **2010**, *31*, 6789−6795.
(26) Lee, J. S.; Ryu, J.; Park, C. B. High-Throughput Analysis of Alzheimer's Beta-Amyloid Aggregation Using a Microfluidic Self-Assembly of Monomers. *Anal. Chem.* **2009**, *81*, 2751−2759.
(27) Knowles, T. P. J.; White, D. A.; Abate, A. R.; Agresti, J. J.; Cohen, S. I. A.; Sperling, R. A.; De Genst, E. J.; Dobson, C. M.; Weitz, D. A. Observation of Spatial Propagation of Amyloid Assembly from Single Nuclei. *Proc. Natl. Acad. Sci. U. S. A.* **2011**, *108*, 14746−14751.
(28) Smith, M. I.; Foderà, V.; Sharp, J. S.; Roberts, C. J.; Donald, A. M. Factors Affecting the Formation of Insulin Amyloid Spherulites. *Colloids Surf., B* **2012**, *89*, 216−222.
(29) Nielsen, L.; Frokjaer, S.; Carpenter, J. F.; Brange, J. Studies of the Structure of Insulin Fibrils by Fourier Transform Infrared (FTIR) Spectroscopy and Electron Microscopy. *J. Pharm. Sci.* **2001**, *90*, 29−37.
(30) Robbins, K. J.; Liu, G.; Lin, G.; Lazo, N. D. Detection of Strongly Bound Thioflavin T Species in Amyloid Fibrils by Ligand-Detected ^{1}H NMR. *J. Phys. Chem. Lett.* **2011**, *2*, 735−740.
(31) Mohanty, J.; Choudhury, S. D.; Pal, H.; Bhasikuttan, A. C. Early Detection of Insulin Fibrillation: a Fluorescence Lifetime Assay to Probe the Pre-Fibrillar Regime. *Chem. Commun.* **2012**, *48*, 2403−2405.
(32) Ricca, M.; Foderà, V.; Giacomazza, D.; Leone, M.; Spadaro, G.; Dispenza, C. Probing the Internal Environment of PVP Networks Generated by Irradiation with Different Sources. *Colloid Polym. Sci.* **2010**, *288*, 969−980.
(33) Bouchard, M.; Zurdo, J.; Nettleton, E. J.; Dobson, C. M.; Robinson, C. V. Formation of Insulin Amyloid Fibrils Followed by FTIR Simultaneously with CD and Electron Microscopy. *Protein Sci.* **2000**, *9*, 1960−1967.
(34) Lee, P.; Lin, R.; Moon, J.; Lee, L. P. Microfluidic Alignment of Collagen Fibers for In Vitro Cell Culture. *Biomed Microdevices* **2006**, *8*, 35−41.
(35) Librizzi, F.; Foderà, V.; Vetri, V.; Lo Presti, C.; Leone, M. Effects of Confinement on Insulin Amyloid Fibrils Formation. *Eur. Biophys. J.* **2007**, *36*, 711−715.
(36) Eggers, D. K.; Valentine, J. S. Molecular Confinement Influences Protein Structure and Enhances Thermal Protein Stability. *Protein Sci.* **2001**, *10*, 250−261.
(37) Sharp, J. S.; Forrest, J. A.; Jones, R. A. L. Surface Denaturation and Amyloid Fibril Formation of Insulin at Model Lipid-Water Interfaces. *Biochemistry* **2002**, *41*, 15810−15819.
(38) Domigan, L. J.; Healy, J. P.; Meade, S. J.; Blaikie, R. J.; Gerrard, J. A. Controlling the Dimensions of Amyloid Fibrils: Toward Homogenous Components for Bionanotechnology. *Biopolymers* **2012**, *97*, 123−133.
(39) Gabrielsson, E. O.; Tybrandt, K.; Hammarström, P.; Berggren, M.; Nilsson, K. P. R. Spatially Controlled Amyloid Reactions Using Organic Electronics. *Small* **2010**, *6*, 2153−2161.